Journal Pre-proof

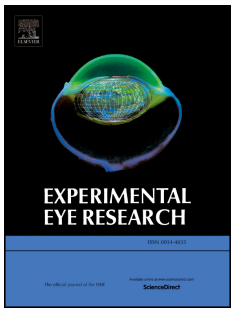

Animal model of subretinal fibrosis without active choroidal neovascularization

Souska Zandi, Yuebing Li, Laura Jahnke, Anelia Schweri-Olac, Keijiro Ishikawa, Iori Wada, Shintaro Nakao, Martin S. Zinkernagel, Volker Enzmann

PII: S0014-4835(23)00049-0

DOI: https://doi.org/10.1016/j.exer.2023.109428

Reference: YEXER 109428

To appear in: *Experimental Eye Research*

Received Date: 28 September 2022

Revised Date: 1 February 2023

Accepted Date: 17 February 2023

Please cite this article as: Zandi, S., Li, Y., Jahnke, L., Schweri-Olac, A., Ishikawa, K., Wada, I., Nakao, S., Zinkernagel, M.S., Enzmann, V., Animal model of subretinal fibrosis without active choroidal neovascularization, *Experimental Eye Research* (2023), doi: https://doi.org/10.1016/j.exer.2023.109428.

Animal Model of Subretinal Fibrosis Without Active Choroidal Neovascularization

Souska Zandi[1], Yuebing Li[1,2], Laura Jahnke[1,2], Anelia Schweri-Olac[1], Keijiro Ishikawa[3], Iori Wada[3], Shintaro Nakao[4], Martin S. Zinkernagel[1], Volker Enzmann[1]

[1] Department of Ophthalmology and Department of BioMedical Sciences, Inselspital, Bern University Hospital, University of Bern, Bern, Switzerland.

[2] Graduate School for Cellular and Biomedical Sciences, University of Bern, Bern, Switzerland

[3] Department of Ophthalmology, Graduate School of Medical Sciences, Kyushu University, Fukuoka, Japan.

[4] Department of Ophthalmology, National Hospital Organization, Kyushu Medical Center, Fukuoka, Japan

Key words: Age-related macular degeneration, CNV, subretinal fibrosis
Running Title: Subretinal fibrosis model

Corresponding Author:
Dr. med. Souska Zandi
INSELSPITAL, Universitätsspital Bern
Universitätsklinik für Augenheilkunde
3010 Bern
Telefon: +41(0)789492904
Email: souskasophie.zandi@insel.ch
ORCID ID: 0000-0001-9351-4278

Abstract

Subretinal fibrosis can occur during neovascular age-related macular degeneration (nAMD) and consequently provokes progressing deterioration of AMD patient`s vision. Intravitreal anti–vascular endothelial growth factor (VEGF) injections decrease choroidal neovascularization (CNV), however, subretinal fibrosis remains principally unaffected. So far, no successful treatment nor established animal model for subretinal fibrosis exists. In order to investigate the impact of anti-fibrotic compounds on solely fibrosis, we refined a time-dependent animal model of subretinal fibrosis without active choroidal neovascularization (CNV). To induce CNV-related fibrosis, wild-type (WT) mice underwent laser photocoagulation of the retina with rupture of Bruch`s membrane. The lesions volume was assessed with optical coherence tomography (OCT). CNV (Isolectin B4) and fibrosis (type 1 collagen) were separately quantified with confocal microscopy of choroidal whole-mounts at every time point post laser induction (day 7-49). In addition, OCT, autofluorescence and fluorescence angiography were carried out at

designated timepoints (day 7, 14, 21, 28, 35, 42, 49) to monitor CNV and fibrosis transformation over time. From 21 to 49 days post laser lesion leakage in the fluorescence angiography decreased. Correspondingly, Isolectin B4 decreased in lesions of choroidal flat mounts and type 1 collagen increased. Fibrosis markers, namely vimentin, fibronectin, alpha- smooth muscle actin (a-SMA) and type 1 collagen were detected at different timepoints of tissue repair in choroids and retinas post laser. These results prove that the late phase of the CNV-related fibrosis model enables screening of anti-fibrotic compounds to accelerate the therapeutic advancement for the prevention, reduction, or inhibition of subretinal fibrosis.

1. Introduction

Age-related macular degeneration (AMD) is a multifactorial disease, with environmental and polygenic components. AMD is the principal cause of adult vision loss and blindness in industrialized countries, of which over 80% are due to choroidal neovascularization (CNV) accompanied by tissue damage and inflammation (Smith et al., 2001; Wong et al., 2008). Subretinal fibrosis can develop during neovascular age-related macular degeneration (nAMD) due to excessive wound healing and consequently deteriorates the vision of AMD patients further.

Angiogenesis is the first step in the process of wound healing as inflammatory cells are recruited to the wounded tissue and the oxygen supply is being increased (Greaves et al., 2013). Infiltration and proliferation of retinal pigment epithelium (RPE), glial cells, fibroblasts, myofibroblasts and macrophages, in addition to secreted cytokines and growth factors result in remodeling of the extracellular matrix (ECM) (Kent and Sheridan, 2003). Myofibroblasts are crucial in the development of ocular fibrosis; numerous

are found in fibrous tissue instigating the excessive synthesis and remodeling of extracellular matrix proteins (Wynn, 2007). Collagen types I, IV and fibronectin (FN) are the most identifiable ECM components in ocular fibrosis tissue (Kimoto et al., 2004). RPE cells that lose their epithelial contacts display an augmented upregulation of mesenchymal markers, including N-cadherin, vimentin and alpha- smooth muscle actin (a-SMA) (Kalluri and Weinberg, 2009). Previous histopathological studies have detected myofibroblasts and a-SMA in human ocular fibrotic tissue (Tamiya and Kaplan, 2016; Lopez et al., 1996; Shu and Lovicu, 2017), their origin can be bone-marrow derived or from RPE cells (Espinosa-Heidmann et al., 2005; Ishikawa et al., 2015).

To date, repeated intraocular injections of vascular endothelial growth factor (VEGF) inhibitors are the most widely used treatment for exudative retinal diseases, namely nAMD, macular edema secondary to retinal vein occlusion (RVO), uveitis and diabetes. Nevertheless, a variety of vitreoretinal responses such as fibrosis in AMD, fibrovascular membrane contraction in diabetic retinopathy (DR) and proliferative vitreoretinopathy (PVR) are not affected by VEGF inhibition alone and are thus limiting the long-term

functional prognosis. Furthermore, there is evidence that VEGF inhibition is linked with the formation of fibrosis in nAMD and proliferative diabetic retinopathy (Van Geest et al., 2012; Barikian et al., 2015).

Hence, novel therapeutic approaches beyond VEGF have – so far unsuccessfully - been researched for the treatment of fibrous scarring of vitreoretinal diseases. Subretinal scarring has been defined as a reason of unsuccessful outcome in nAMD patients in a large amount of anti-VEGF treated eyes (Daniel et al., 2014) and currently, no successful treatment for subretinal fibrosis exists. Therefore, a screening method for effective therapeutic and preventive measures of ocular fibrosis is urgently needed. This work introduces a time-dependent animal model of subretinal fibrosis.

2. Materials & Methods

2.1 Animals

Experiments were performed with adult male and female C57BL/6J mice (Charles River Germany), 8 -12 weeks old, weighing 20 to 25 g. Animals were housed in individually ventilated cages (IVC). The temperature-controlled animal facility is equipped with a 12-hour light/dark cycle. Mice were fed standard laboratory chow and water *ad libitum*. The Animal Experimentation Committee of the Canton of Bern (BE 146/2020) approved experimental protocols.

2.2 Laser-induced CNV

C57BL/6 mice were anesthetized, pupils were dilated and cornea kept hydrated as described in detail previously (Kokona et al., 2018; Schwarzer et al., 2020). In order to induce the lesions, a 532-nm diode laser (Visulas 532s; Carl Zeiss Meditec AG, Oberkochen, Germany) and a cover glass as a

125 contact lens were utilized to place six spots (100 mW, 50 µm, 100 ms) in each
126 eye. The lesions were located at about 2 disk diameters from the optic
127 nerve head. The rupture of Bruch's membrane was valided by the
128 emergence of a bubble. At the occurence of hemorrhage, eyes were
129 excluded.
130

131 **2.3 Quantification of CNV and fibrosis**

132 On designated time points (d7, d14, d21, d28, d35, d42 and d49) post laser,
133 the volume of CNV lesions and subretinal fibrosis was quantified in optical
134 coherence tomography (OCT; Heidelberg Spectralis HRA2, Heidelberg
135 Engineering GmbH, Heidelberg, Germany), and additionally after euthanasia
136 and eye removal in choroidal flat mounts (Zeiss LSM 710 laser scanning
137 confocal microscope). Flat mount preparation was performed as described
138 in detail previously (Nakao et al., 2013; Zandi et al., 2015). The flat mounts
139 were stained for CNV (isolectin GS-IB4; I21411, life technologies, dilution
140 1:200) and fibrosis (anti-collagen 1 antibody; MA1-26771 Invitrogen, dilution
141 1:200).

The OCT volume measurements were carried out according to the previously published method (Sulaiman et al., 2015) and the size of CNV and fibrotic lesions of the flat mounts was separately evaluated by quantifying the hyperfluorescent area with Fiji/Image J Software (Version 2.1.0/1.53c). Furthermore, autofluorescence (AF) and fluorescence angiography (FA) were conducted every week post laser (week 1 to week 7) aiming to assess CNV and fibrosis changes over time. The amount of leakage was graded by FA.

2.4 Fluorescein angiography

FA was carried out in anesthetized mice after pupil dilation using a digital fundus camera (SLO; HRA2; Heidelberg Engineering), on all designated time points post laser induction. Fluorescein injections were administered subcutaneously with 50 µL of 0.01% fluorescein (Faure; Novartis, Basel, Switzerland) and diluted in phosphate buffered saline (PBS). OCT, AF and FA

images were acquired and assessed by two masked retina specialists. The FA grading criteria were as described in detail previously (Zandi et al., 2015).

2.5 Fundus Autofluorescence Imaging

After anesthesia and pupil dilation autofluorescence images were acquired using an ultrawide field 102-degree lens (Heidelberg Engineering). Application of Methocel 2% helped to keep eyes moist and impeded drying of the cornea.

2.6 Immunohistochemistry

On day 7, 14, 21, 28, 35, 42 and 49 post laser 10µm sections of the posterior segment were obtained after eyes were fixated in 4% paraformaldehyde solution at 4°C for 24 hours. The mouse eye sections were stained with hematoxylin and eosin (HE) or incubated with anti-collagen 1 antibody

(MA1-26771 Invitrogen, dilution 1:100) and isolectin GS-IB4 (I21411, life technologies, dilution 1:100) or anti-a-SMA antibody (ab15734; Abcam, dilution 1:100), and thereafter with the secondary Ab (dilution 1:500). Images were obtained with a scanning laser microscope (Carl Zeiss Microscopy and Leica Microsystems).

2.7 Western Blot

For western blot, 10 laser spots (100 mW, 50 µm, 100 ms) were placed in each eye. To obtain tissues, the retina and the choroid-RPE complex were micro-surgically isolated following enucleation of eyes. Thenceforth the retina and RPE-choroid complex were separately placed in 100 µl of lysis buffer (Table 1), supplemented with protease (MG-132; 474790, Calbiochem) and phosphatase inhibitors (P2850 Sigma-Aldrich), as well as protease inhibitor cocktail (cOmplete ULTRA Tablets, EDTA-free; Roche, Basel, Switzerland). Subsequently, lysed samples were homogenized with a Precellys 24 tissue homogenizer (Bertin Instruments, Montigny-le-Bretonneux, France) and

centrifuged at 5000g and 4 °C for 1 minute. The supernatant was transferred to another Eppendorf tube and then again centrifuged at 13000 rpm and 4 °C for 20 minutes. After collection of the supernatants the samples were stored at -80°C. Each sample with an equal amount of total protein, previously quantified by protein assay (Coomassie Plus, Bradford Assay Kit, 23236, Pierce™), was separated by SDS-PAGE and electroblotted to Trans-Blot Turbo Mini 0.2 µm Nitrocellulose Transfer Packs membranes (1704158; BIO-RAD). To block nonspecific binding, the membranes were washed with Blocking Buffer TBS (LIC-927-60001: LI-COR) and subsequently incubated with the following: rabbit or mouse Abs against collagen 1 (MA1-26771; Invitrogen, dilution 1:500), fibronectin(ab2413; Abcam, dilution 1:1000), vimentin (NBP1-97672; NOVUS, dilution 1:100), α-SMA (ab15734; Abcam, dilution 1:1000) and beta-actin (161-0373; BIO-RAD, dilution 1:1000) at 4°C overnight, followed by incubation with 680RD Donkey anti-Mouse IgG Secondary Antibody(926-68072; IRDye®, LI-COR) or 800CW Donkey anti-Rabbit IgG Secondary Antibody(926-32213; IRDye®, LI-COR). The signals were visualized by fluorescence (LI-COR Odyssey Infrared Imaging System).

204 **Table1** Composition of lysis buffer

Ingredients	Concentration
Tris-HCl (pH 7.5)	20 mM
NaCl	150 mM
EDTA	5 mM
Na-Pyrophosphate	5 mM
NaH_2PO_4 (pH7.6)	20 mM
Na-β-glycerophosphate	3 mM
NaF	10 mM

205

206 **2.8 Statistical analysis**

207 In accordance with the Shapiro-Wilk test our data were normally distributed.

208 As a result, the data were analyzed by two-tailed *t*-test or ANOVA.

209 All values are displayed as mean ± standard error of the mean (SEM).

210 Disparities between groups were considered statistically significant (*), when

211 the probability value, *P* was <0.05. All statistical analyses were performed

212 with Excel (version 16.64) and R (package FSA, version 3.4.0).

213

214

215 # 3. Results

216

217 ## 3.1 Subretinal fibrosis development over time

218 Autofluorescence (AF), fluorescein angiography (FA) and optical coherence
219 tomography (OCT) images of the same mouse fundus over designated time
220 points together with representative flat mounts (FM), stained with isolectin B4
221 for choroidal neovascularization and type 1 collagen for fibrosis, clearly
222 demonstrate the increase of fibrosis and the reduction of active CNV over
223 time **(Fig. 1A)**. To visualize this effect, we chose live images from the same
224 mouse eye every week from 7 to 49 days post laser induction of the lesions.
225 The quantification of the lesion volume with OCT measurements on all
226 designated time points of 60 lesions of10 eyes of 6 mice showed the same
227 trend. Two eyes of the 12 eyes of the 6 mice were excluded due to
228 hemorrhages. However, a significant difference was only seen when
229 comparing day 7 to day 21. Here we can see a significant reduction in lesion
230 size, whereas the other time-points did not differ significantly in lesion volume.
231 This finding can be explained as we look at the volume of the live image in

OCT, where the CNV volume reduces with time, but the fibrotic one increases **(Fig. 1B)**. This fact becomes obvious when looking at Figure 1c, d and e. Active CNV peaks on day 7 whereupon it starts to regress and almost entirely disappears within 35 to 49 days after laser injury **(Fig. 1C)**. The CNV volume also subsides significantly from day 21 on **(Fig. 1D)**. In contrast, fibrous tissue starts increasing from 21 days post laser treatment and continues to expand until 49 days after laser injury **(Fig. 1E)**. Over a considerable length of time we here assessed an alteration of CNV and fibrous tissue development in the laser-induced CNV mouse model in line with the previous findings of Ishikawa et al. (Ishikawa et al., 2015; Ishikawa et al., 2016), mimicking the clinical changes of patients with nAMD where subretinal fibrosis occurs subsequently to CNV.

3.2 Alpha-SMA and type 1 collagen expression in CNV/subretinal fibrosis lesions

HE staining of the retinal-choroidal complexes depict the laser-induced lesion with rupture of Bruch`s membrane **(Fig. 2A)**.

Immunostaining showed an increase of type 1 collagen, an extracellular matrix protein that is present in scars, from day 21 after CNV induced fibrosis. Alpha-SMA, a marker for activated myofibroblasts, was reduced in comparison to the first two weeks after lesion induction and increased again from 35 days after laser-induced CNV **(Fig. 2A, B)**.

3.3 Development of fibrosis after CNV

To investigate the time-dependent change of CNV and fibrosis we screened the retina and the RPE-choroid complex separately for fibrosis markers, such as type 1 collagen, fibronectin, vimentin and a-SMA. In the RPE-choroid complex, we could detect an increase of vimentin, a-SMA and type 1 collagen one week post laser and another peak 28 to 42 days after CNV induced fibrosis **(Fig. 3A, B, C, E)**. However, type 1 collagen together with fibronectin were the only fibrosis markers with the highest peak 35 days post laser **(Fig. 3 A, B, D)**. Besides vimentin, an intermediate filament (IF) protein, which peaked significantly 7 days post laser, all other fibrosis markers we screened in choroids of 6 eyes of 3 mice were significantly increased at

day 35 or 42 post laser **(Fig. 3)**. Vimentin is an important cytoskeletal component and marker of mesenchymal-derived cells and cells going through epithelial-mesenchymal transition. Obviously, it is increased one week post laser as tissue injury initiates the common steps of wound healing with the transition of fibroblasts to myofibroblasts and scar-forming extracellular matrix reorganization. Type 1 collagen and a-SMA also peak 7 days post injury and are then again enhanced 5- and 6-weeks post laser **(Fig. 3 A, B, C)**. Interestingly, fibronectin, a glycoprotein that mediates the attachment of fibroblasts to the extracellular matrix, decreased significantly two- and three-weeks post laser and increased substantially 5 weeks post laser **(Fig. 3 A, D)**. As myofibroblasts express a-SMA to form stress fibers and increase the capacity to synthesize collagens, fibronectin, and other ECM components in the wound healing process, it explains, that a-SMA is expressed earlier in the RPE-choroid complex post laser than fibronectin **(Fig. 3 A, B)**.

In line with our immunostaining of the retinal-choroidal complexes **(Fig.2)**, a-SMA is again significantly upregulated 7 to14 days in retinas of lasered mice

eyes (n=6 eyes; 3 mice) with another peak after 4 to 6 weeks post laser **(Fig. 4 A, C)**. In line with our findings in the RPE-choroid complex, type 1 collagen and fibronectin show a peak 5 weeks after CNV-induced fibrosis, however they are not significantly upregulated in the early stage of wound healing **(Fig. 4 A, B, D)**. Interestingly, vimentin is expressed higher in the late stage of wound repair in lasered retinas, opposed to our findings in the choroid **(Fig. 4 A, E)**.

4. Discussion

AMD management is a public health priority and anti-VEGF treatment of choroidal neovascularization is regularly administered in exudative AMD. However, the pathogenesis of subretinal fibrosis in AMD is not well understood and no cure or prevention currently exists. Here, we established a time-dependent animal model of subretinal fibrosis in order to enable screening for anti-fibrotic compounds.

Type I collagen is increased 21 to 35 days after CNV induction; at the same time, a gain in subretinal fibrosis and a decrease in active CNV with reduced to completely vanished leakage in the fluorescence angiography images was detectable.

To investigate the pathogenesis and explore treatment options for nAMD an extensive amount of animal models has been applied (Grossniklaus et al., 2010); however, models that explicitly scrutinize subretinal fibrosis are sparse. A well-established animal model for neovascular AMD research is the laser induced CNV mouse model (Ishibashi et al., 1987; Tobe et al., 1998). In this model, RPE is injured with laser resulting in rupture of Bruch's membrane,

317 which initiates an acute inflammatory response with recruitment of immune
318 cells, and the consequent formation of CNV. Several studies have explored
319 the underlying molecular mechanisms and new therapeutic targets for
320 choroidal neovascularization in the early stage, mainly from day 3 to day 14
321 (Apte et al. 2006; Noda et al., 2008; Zandi et al.,2015). Ishikawa et al.,
322 however, suggested that particularly the late stage of the CNV model serves
323 the study of mechanisms of subretinal fibrosis. In the late phase, evaluation of
324 fibrosis-related molecular changes can be investigated, regardless of the
325 impact of concurrent active CNV (Ishikawa et al., 2015; Ishikawa et al., 2016).
326 Little et al. recently introduced a laser-induced mouse model of subretinal
327 fibrosis whereupon a second laser burn is applied to the CNV lesion after one
328 week. These lesions exist of CNV, fibrosis and hemorrhage, all of which are
329 implicated in the inflammatory and fibrotic pathways (Little et al., 2020).
330 Therefore, distinction between fibrosis and CNV seems to be impossible in
331 that animal model and mechanisms of anti-fibrotic agents might not
332 uniquely be attributed to changes in fibrosis when CNV and hemorrhage are
333 present. These induced subretinal fibrovascular membranes are bigger and

interesting for studies of fibrovascular tissue [22]. However, to examine the effect of anti-fibrotic agents, we believe a subretinal fibrosis model without active CNV is beneficial. Therefore, we established a distinct fibrosis model, first postulated by Ishikawa et al. (Ishikawa et al., 2015; Ishikawa et al., 2016). In our long-term fibrosis model, we can show with fluorescence angiography that CNV is not active from 21 to 49 days post laser, nevertheless, fibrosis increases from that time point (day 21) on.

Concerns arise regarding some of the already existing animal models for subretinal fibrosis with respect to the complexity of those models. First and foremost, multiple steps are needed, including peritoneal macrophage collection and subretinal injection to the bleb after photocoagulation to rupture Bruch`s membrane (Jo et al., 2011) or repeated laser burns on the already existing CNV lesions (Little et al., 2020), with questionable reproducibility of those models. Both models lead subsequently to the formation of fibrovascular lesions, with active CNV and fibrosis. Interestingly, *vldlr* $^{-/-}$ (very-low-density lipoprotein receptor) knockout mice have been

350 described to spontaneously develop subretinal neovascularization and
351 retinal angiomatous proliferation (RAP) like lesions with consequently
352 subretinal fibrosis. Changes in the wnt pathway and initial retinal, not
353 choroidal neovascularization were being observed (Hu et al., 2008; Chen et
354 al., 2020). The incidence of scar formation in these types of lesions originating
355 from the retinal not choroidal vasculature is relatively low as the RPE is less
356 affected than in classic or and occult lesions (Tenbrock et al., 2022).

357 Initial CNV is an important factor in subretinal fibrosis development. Tissue
358 injury first leads to inflammation, with consequently epithelial-mesenchymal
359 transition (EMT) of fibroblasts, converting to myofibroblasts (Wynn, 2007; Kalluri
360 and Weinberg, 2009). Neovascularization then results in the process of wound
361 healing and fibrosis by increasing the population of inflammatory cells,
362 fibroblasts, myofibroblasts and assembly of extracellular matrix proteins,
363 subsequently causing a fibrotic scar. Subretinal fibrosis can then lead to visual
364 loss due to impairment of the RPE and photoreceptors. It has been previously
365 reported that the progression of photoreceptor destruction is proportional to

366 the extent of subretinal fibrosis in histopathologic results of human AMD eyes
367 (Green and Enger, 1993).

368 Macrophages, among others, regulate fibrosis by producing extracellular
369 matrix proteins, particularly type 1 collagen and fibronectin (Gratchev et al.,
370 2001; Vaage and Lindblad, 1990), as well as producing pro-fibrotic
371 mediators, namely, Transforming growth gactor β (TGF-β) and Platelet-
372 derived growth factor (PDGF) (Wynn and Barron, 2010). However, these
373 immune cells can also reverse fibrosis by secreting matrix metalloproteinases
374 (MMPs) and to that end promoting extracellular matrix decomposition (Skeie
375 and Mullins, 2009). Our data show that vimentin is playing a role in early
376 wound healing in the RPE-choroid complex, and that a-SMA and type 1
377 collagen show a two peak wave dynamic, however, fibronectin appears
378 later in the fibrotic wound repair. We can detect a significant increase in
379 fibronectin at day 35 after laser injury in the choroid and retina, however at
380 day 28 and 42 we do not observe a substantial increase. As the fibronectin
381 assembly is a dynamic, spatial, and temporal process, we do believe that

382 this fact may explain the individual differences we see in our data obtained
383 from western blotting. In addition, different forms of fibronectin, such as
384 plasma and cellular FN play distinct roles during various stages of tissue
385 repair, which could further explain the observed differences (Stoffels et al.
386 2013; To and Midwood, 2011).
387 Chronic wound healing may result in excessive fibronectin degradation,
388 causing abnormal healing with augmentation of the scar tissue. Fibronectin is
389 degraded to create place for collagen deposition (Patten and Wang, 2021;
390 Lenselink et al., 2015, Broughton et al., 2006). We can observe a significant
391 increase in type-1collagen at day 35 and 42 post laser in the choroid. This
392 could explain the degradation of fibronectin at day 42 and significant
393 increase of collagen 1. Its remodeling may continue for a long time after
394 wound closure depending on the tissue. Matrix metalloproteinases (MMPS)
395 are key components in collagen degradation (Caley et al., 2015); however,
396 the complexity of the subject matter in the retina and choroid requires future
397 insights to be fully understood.

The immune response in AMD and subretinal fibrosis is complex. This becomes even more obvious when considering the limited influence of anti-inflammatory agents, namely steroids for nAMD (Ambati et al., 2013). One research focus to date are therapeutic options for the prevention, reduction and inhibition of subretinal fibrosis. Several studies proposed that VEGF inhibition for nAMD may likewise hinder subretinal fibrosis`s evolution or progression (Bloch et al., 2013; Luo et al., 2013). In contrast, it has been reported that fibrosis develops after VEGF inhibition in eyes with nAMD or proliferative diabetic retinopathy (PDR) (Van Geest et al., 2012; Barikian et al., 2015; Hwang et al., 2013; Arevalo et al., 2008). A prospective cohort study observed that "classic" CNV lesions in eyes of nAMD patients show a higher degree of scar formation than "occult" ones, when treated previously with VEGF inhibition (Daniel et al., 2014).

The findings of histopathologic studies of human CNV membranes indicate that subretinal fibrosis advances with reduction of CNV in nAMD (Hinton et al., 1998), which is well in line with our findings that show long-lasting CNV but

low vascular permeability. As of yet, neovascular or fibrotic membranes of AMD patients are not anymore surgically obtained, therefore, animal models that mimic the human course of subretinal fibrosis are urgently needed (Tenbrock et al., 2022).

4.1. Conclusions

We assessed a modification of CNV and fibrosis in the laser-induced CNV mouse model over time. In that model, active CNV peaks between day 7 to 14, after which its regression begins and almost entirely fades from 21 to 35 days post laser. Interestingly, we remarked that fibrosis continues to expand for over 35 days post laser treatment. This model mimics the natural process of nAMD eyes of patients, where subretinal fibrous scarring happens after CNV. We postulate this model as a well-functioning animal model for subretinal fibrosis without active CNV in the late stage and believe that the advanced phase of the laser induced CNV model will be helpful for understanding and investigating the pathophysiology of solely subretinal fibrosis.

The current results indicate that the here introduced time-dependent model of fibrosis allows for screening of anti-fibrotic treatment and will likely lead to urgently needed novel therapeutics for subretinal fibrosis after neovascular age-related macular degeneration and further fibrotic diseases of the eye and other organs.

Acknowledgement

We thank Prashanthni Sivapatham and Sophia Morandi for their remarkable technical assistance.

Competing interests

Martin S Zinkernagel acts as a consultant for Heidelberg Engineering. The remaining authors have no financial/proprietary interests.

Funding

This research did not receive any specific grant from funding agencies in the public, commercial, or not-for-profit sectors.

References

Ambati J, Atkinson JP, Gelfand BD. (2013). Immunology of age-related macular degeneration. Nature reviews. Immunology. 2013; 13:438–451. [PubMed: 23702979]

Apte RS, Richter J, Herndon J, Ferguson TA. (2006). Macrophages inhibit neovascularization in a murine model of age-related macular degeneration. PLoS Med. 2006 Aug;3(8):e310. doi: 10.1371/journal.pmed.0030310. PMID: 16903779; PMCID: PMC1539093.

Arevalo JF, Maia M, Flynn HW Jr, Saravia M, Avery RL, Wu L, Eid Farah M, Pieramici DJ, Berrocal MH, Sanchez JG. (2008). Tractional retinal detachment following intravitreal bevacizumab (Avastin) in patients with severe proliferative diabetic retinopathy. Br J Ophthalmol. 2008; 92:213–216. [PubMed: 17965108]

Barikian A, Mahfoud Z, Abdulaal M, Safar A, Bashshur ZF: (2015). Induction with intravitreal bevacizumab every two weeks in the management of neovascular age-related macular degeneration. Am J Ophthalmol 2015, 159:131e137

Bloch SB, Lund-Andersen H, Sander B, Larsen M. (2013). Subfoveal fibrosis in eyes with neovascular age- related macular degeneration treated with intravitreal ranibizumab. Am J Ophthalmol. 2013; 156:116–124. e111. [PubMed: 23664150]

Broughton G 2nd, Janis JE, Attinger CE. (2006). The basic science of wound healing. Plast Reconstr Surg. 2006 Jun;117(7 Suppl):12S-34S. doi: 10.1097/01.prs.0000225430.42531.c2. PMID: 16799372.

Caley, M.P., Martins, V. L. & O'Toole, E.A. (2015). Metalloproteinases and Wound Healing. *Adv Wound Care (New Rochelle)* **4**, 225-234, doi:10.1089/wound.2014.0581.

Chen Q, Jiang N, Zhang Y, Ye S, Liang X, Wang X, Lin X, Zong R, Chen H, Liu Z. (2020). Fenofibrate Inhibits Subretinal Fibrosis Through Suppressing TGF-β-Smad2/3 signaling and Wnt signaling in Neovascular Age-Related Macular Degeneration. Front Pharmacol. 2020 Nov 17;11:580884. doi: 10.3389/fphar.2020.580884. PMID: 33442383; PMCID: PMC7797782.

Daniel E, Toth CA, Grunwald JE, Jaffe GJ, Martin DF, Fine SL, Huang J, Ying GS, Hagstrom SA, Winter K, Maguire MG; (2014). Comparison of Age-related Macular Degeneration Treatments Trials Research Group. Risk of scar in the comparison of age-related macular degeneration treatments trials. Ophthalmology. 2014 Mar;121(3):656-66.

Espinosa-Heidmann DG, Reinoso MA, Pina Y, Csaky KG, Caicedo A, Cousins SW: (2005). Quantitative enumeration of vascular smooth muscle cells and endothelial cells derived from bone marrow precursors in experimental choroidal neovascularization. Exp Eye Res 2005, 80:369e378

Gratchev A, Guillot P, Hakiy N, Politz O, Orfanos CE, Schledzewski K, Goerdt S. (2001). Alternatively activated macrophages differentially express fibronectin and its splice variants and the extracellular matrix protein betaIG-H3. Scandinavian journal of immunology. 2001; 53:386–392. [PubMed: 11285119]

Greaves NS, Ashcroft KJ, Baguneid M, Bayat A. (2013). Current understanding of molecular and cellular mechanisms in fibroplasia and angiogenesis during acute wound healing. Journal of dermatological science. 2013; 72:206–217. [PubMed: 23958517]

Green WR, Enger C. (1992). Age-related macular degeneration histopathologic studies. The 1992 Lorenz E. Zimmerman Lecture. Ophthalmology. 1993; 100:1519–1535. [PubMed: 7692366]

Grossniklaus HE, Kang SJ, Berglin L. (2010). Animal models of choroidal and retinal neovascularization. Prog Retin Eye Res. 2010 Nov;29(6):500-19. doi: 10.1016/j.preteyeres.2010.05.003. Epub 2010 May 19. PMID: 20488255; PMCID: PMC2962694.

Hinton DR, He S, Lopez PF. (1998). Apoptosis in surgically excised choroidal neovascular membranes in age- related macular degeneration. Arch Ophthalmol. 1998; 116:203–209. [PubMed: 9488273]

Hu W, Jiang A, Liang J, Meng H, Chang B, Gao H, Qiao X. (2008). Expression of VLDLR in the retina and evolution of subretinal neovascularization in the knockout mouse model's retinal angiomatous proliferation. Invest Ophthalmol Vis Sci. 2008 Jan;49(1):407-15. doi: 10.1167/iovs.07-0870. PMID: 18172119.

Hwang JC, Del Prire LV, Freund KB, Chang S, Iranmanesh R. (2011). Development of subretinal fibrosis after anti-VEGF treatment in neovascular age-related macular degeneration. Ophthalmic Surg Lasers Imaging. 2011; 42:6–11. [PubMed: 20954648]

Ishibashi, T., Miller, H., Orr, G., Sorgente, N., and Ryan, S.J. (1987). Morpho- logic observations on experimental subretinal neovascularization in the mon- key. Invest. Ophthalmol. Vis. Sci. *28*, 1116–1130.

Ishikawa K, Kannan R, Hinton DR. (2015). Molecular mechanisms of subretinal fibrosis in age-related macular degeneration. Exp Eye Res. 2016 Jan;142:19-25. doi: 10.1016/j.exer.2015.03.009. Epub 2015 Mar 13. PMID: 25773985; PMCID: PMC4568171.

Ishikawa K, Sreekumar PG, Spee C, Nazari H, Zhu D, Kannan R, Hinton DR. (2016). αB-Crystallin Regulates Subretinal Fibrosis by Modulation of Epithelial-Mesenchymal Transition. Am J Pathol. 2016 Apr;186(4):859-73. doi: 10.1016/j.ajpath.2015.11.014. Epub 2016 Feb 12. PMID: 26878210; PMCID: PMC4822331.

Jo YJ, Sonoda KH, Oshima Y, Takeda A, Kohno R, Yamada J, Hamuro J, Yang Y, Notomi S, Hisatomi T, Ishibashi T. (2011). Establishment of a new animal model of focal subretinal fibrosis that resembles disciform lesion in advanced age-related macular degeneration. Invest Ophthalmol Vis Sci. 2011 Aug 1;52(9):6089-95. doi: 10.1167/iovs.10-5189. PMID: 21051730.

Kalluri R, Winberg RA. (2009). The basics of epithelial-mesenchymal transition. J Clin Invest. 2009 Jun;119(6):1420-8. doi: 10.1172/JCI39104. Erratum in: J Clin Invest. 2010 May 3;120(5):1786. PMID: 19487818; PMCID: PMC2689101.

Kent D, Sheridan C. (2003). Choroidal neovascularization: a wound healing perspective. Mol Vis. 2003; 9:747–755. [PubMed: 14735062]

Kimoto K, Nakatsuka K, Matsuo N, Yoshioka H. (2004). p38 MAPK mediates the expression of type I collagen induced by TGF-beta 2 in human retinal pigment epithelial cells ARPE-19. Invest Ophthalmol Vis Sci. 2004 Jul;45(7):2431-7. doi: 10.1167/iovs.03-1276. PMID: 15223827.

Kokona D, Ebneter A, Escher P, Zinkernagel MS. (2018). Colony-stimulating factor 1 receptor inhibition prevents disruption of the blood-retina barrier during chronic inflammation. J Neuroinflammation. 2018 Dec 12;15(1):340. doi: 10.1186/s12974-018-1373-4. PMID: 30541565; PMCID: PMC6292111.

Lenselink EA. (2013). Role of fibronectin in normal wound healing. Int Wound J. 2015 Jun;12(3):313-6. doi: 10.1111/iwj.12109. Epub 2013 Jun 7. PMID: 23742140; PMCID: PMC7950333.

Little K, Llorián-Salvador M, Tang M, Du X, O'Shaughnessy Ó, McIlwaine G, Chen M, Xu H. (2020). A Two-Stage Laser-Induced Mouse Model of Subretinal Fibrosis Secondary to Choroidal Neovascularization. Transl Vis Sci Technol. 2020 Mar 9;9(4):3. doi: 10.1167/tvst.9.4.3. PMID: 32818091; PMCID: PMC7396176.

Lopez PF, Sippy BD, Lambert HM, Thach AB, Hinton DR. (1996). Transdifferentiated retinal pigment epithelial cells are immunoreactive for vascular endothelial growth factor in surgically excised age-related macular degeneration-related choroidal neovascular membranes. Invest Ophthalmol Vis Sci. 1996 Apr;37(5):855-68. PMID: 8603870.

Luo L, Zhang X, Hirano Y, Tyagi P, Barabás P, Uehara H, Miya TR, Singh N, Archer B, Qazi Y, Jackman K, Das SK, Olsen T, Chennamaneni SR, Stagg BC, Ahmed F, Emerson L, Zygmunt K, Whitaker R, Mamalis C, Huang W, Gao G, Srinivas SP, Krizaj D, Baffi J, Ambati J, Kompella UB, Ambati BK. (2013). Targeted intraceptor nanoparticle therapy reduces angiogenesis and fibrosis in primate and murine macular degeneration. ACS Nano. 2013 Apr 23;7(4):3264-75. doi: 10.1021/nn305958y. Epub 2013 Mar 20. PMID: 23464925; PMCID: PMC3634882.

Nakao S, Zandi S, Kohno R, Sun D, Nakama T, Ishikawa K, Yoshida S, Enaida H, Ishibashi T, Hafezi-Moghadam A. (2013). Lack of lymphatics and lymph node-mediated immunity in choroidal neovascularization. Invest Ophthalmol Vis Sci. 2013 Jun 3;54(6):3830-6. doi: 10.1167/iovs.12-10341. Erratum in: Invest Ophthalmol Vis Sci. 2013 Jul;54(7):4451. PMID: 23580489; PMCID: PMC3671933.

Noda K, She H, Nakazawa T, Hisatomi T, Nakao S, Almulki L, Zandi S, Miyahara S, Ito Y, Thomas KL, Garland RC, Miller JW, Gragoudas ES, Mashima Y, Hafezi-Moghadam A. (2008). Vascular adhesion protein-1 blockade suppresses choroidal neovascularization. FASEB J. 2008 Aug;22(8):2928-35. doi: 10.1096/fj.07-105346. Epub 2008 Apr 24. PMID: 18436961; PMCID: PMC2493453.

Patten J, Wang K. (2021). Fibronectin in development and wound healing. Adv Drug Deliv Rev. 2021 Mar;170:353-368. doi: 10.1016/j.addr.2020.09.005. Epub 2020 Sep 19. PMID: 32961203.

Schwarzer P, Kokona D, Ebneter A, Zinkernagel MS. (2019). Effect of Inhibition of Colony-Stimulating Factor 1 Receptor on Choroidal Neovascularization in Mice. Am J Pathol. 2020 Feb;190(2):412-425. doi: 10.1016/j.ajpath.2019.10.011. Epub 2019 Nov 26. PMID: 31783006.

Shu DY, Lovicu FJ. (2017). Myofibroblast transdifferentiation: The dark force in ocular wound healing and fibrosis. *Prog Retin Eye Res*. 2017;60:44-65. doi:10.1016/j.preteyeres.2017.08.001

Smith W, Assink J, Klein R, Mitchell P, Klaver CC, Klein BE, Hofman A, Jensen S, Wang JJ, de Jong PT. (2001).Risk factors for age-related macular degeneration: Pooled findings from three continents. Ophthalmology. 2001 Apr;108(4):697-704. doi: 10.1016/s0161-6420(00)00580-7. PMID: 11297486.

Skeie JM, Mullins RF. (2009). Macrophages in neovascular age-related macular degeneration: friends or foes? Eye (Lond). 2009; 23:747–755. [PubMed: 18600240]

Stoffels JM, Zhao C, Baron W. (2013). Fibronectin in tissue regeneration: timely disassembly of the scaffold is necessary to complete the build. Cell Mol Life Sci. 2013 Nov;70(22):4243-53. doi: 10.1007/s00018-013-1350-0. Epub 2013 Jun 12. PMID: 23756580.

Sulaiman RS, Quigley J, Qi X, O'Hare MN, Grant MB, Boulton ME, Corson TW. (2015). A Simple Optical Coherence Tomography Quantification Method for Choroidal Neovascularization. J Ocul Pharmacol Ther. 2015 Oct;31(8):447-54. doi: 10.1089/jop.2015.0049. Epub 2015 Jun 10. PMID: 26060878; PMCID: PMC4598937.

Tamiya S, Kaplan HJ. (2016). Role of epithelial-mesenchymal transition in proliferative vitreoretinopathy. Exp Eye Res. 2016 Jan;142:26-31. doi: 10.1016/j.exer.2015.02.008. PMID: 26675400.

Tenbrock L, Wolf J, Boneva S, Schlecht A, Agostini H, Wieghofer P, Schlunck G, Lange C. (2022). Subretinal fibrosis in neovascular age-related macular degeneration: current concepts, therapeutic avenues, and future perspectives. Cell Tissue Res. 2022 Mar;387(3):361-375. doi: 10.1007/s00441-021-03514-8. Epub 2021 Sep 3. PMID: 34477966; PMCID: PMC8975778.

To WS, Midwood KS. (2011). Plasma and cellular fibronectin: distinct and independent functions during tissue repair. Fibrogenesis Tissue Repair. 2011 Sep 16;4:21. doi: 10.1186/1755-1536-4-21. PMID: 21923916; PMCID: PMC3182887.

Tobe T, Ortega S, Luna JD, Ozaki H, Okamoto N, Derevjanik NL, Vinores SA, Basilico C, Campochiaro PA. (1998). Targeted disruption of the FGF2 gene does not prevent choroidal neovascularization in a murine model. Am J Pathol. 1998 Nov;153(5):1641-6. doi: 10.1016/S0002-9440(10)65753-7. PMID: 9811357; PMCID: PMC1853405.

Vaage J, Lindblad WJ. (1990). Production of collagen type I by mouse peritoneal macrophages. J Leukoc Biol. 1990; 48:274–280. [PubMed: 2202772]

Van Geest RJ, Lesnik-Oberstein SY, Tan HS, Mura M, Goldschmeding R, Van Noorden CJ, Klaassen I, Schlingemann RO: (2012). A shift in the balance of vascular endothelial growth factor and connective tissue growth factor by bevacizumab causes the angiofibrotic switch in proliferative diabetic retinopathy. Br J Ophthalmol 2012, 96:587e590

Wong TY, Chakravarthy U, Klein R, Mitchell P, Zlateva G, Buggage R, Fahrbach K, Probst C, Sledge I. (2008). The natural history and prognosis of neovascular age-related macular degeneration: a systematic review of the literature and meta-analysis. Ophthalmology. 2008 Jan;115(1):116-26. doi: 10.1016/j.ophtha.2007.03.008. Epub 2007 Aug 6. Erratum in: Ophthalmology. 2008 Sep;115(9):1524. Wong, Tien [corrected to Wong, Tien Y]. PMID: 17675159.

Wynn TA. (2007). Common and unique mechanisms regulate fibrosis in various fibroproliferative diseases. J Clin Invest. 2007; 117:524–529. [PubMed: 17332879]

Wynn TA, Barron L. (2010). Macrophages: master regulators of inflammation and fibrosis. Seminars in liver disease. 2010; 30:245–257. [PubMed: 20665377]

Zandi S, Nakao S, Chun KH, Fiorina P, Sun D, Arita R, Zhao M, Kim E, Schueller O, Campbell S, Taher M, Melhorn MI, Schering A, Gatti F, Tezza S, Xie F, Vergani A, Yoshida S, Ishikawa K, Yamaguchi M, Sasaki F, Schmidt-Ullrich R, Hata Y, Enaida H, Yuzawa M, Yokomizo T, Kim YB, Sweetnam P, Ishibashi T, Hafezi-Moghadam A. (2015). ROCK-isoform-specific polarization of macrophages associated with age-related macular degeneration. Cell Rep. 2015 Feb

632 24;10(7):1173-86. doi: 10.1016/j.celrep.2015.01.050. Epub 2015 Feb 19. PMID: 25704819;
633 PMCID: PMC5219927.

634

635

636

637

638

639

640

641

642

643

644

645

646

647

648

649 ## Legends

650

651 **Figure 1: *In vivo* imaging of subretinal fibrosis development over time**

652 **A)** Representative autofluorescence (AF), fluorescein angiography (FA) and
653 optical coherence tomography (OCT) images of the same mouse fundus
654 over designated time points and representative flat mounts (FM) stained with
655 isolectin B4 (green) and type 1 collagen (red). Yellow dashed circle shows
656 the extent of the CNV lesions filled with fluorescein and the corresponding
657 lesion in AF. Yellow arrow points to the subretinal fluid in the OCT image of
658 day 7 after laser injury. Scale bar represents 100 μm. **B)** Quantification of the
659 lesion volume on all designated time points (n=60 lesions of 10 eyes of 6 mice
660 per time point). **C)** Leakage from the angiogenic vessels was visualized by FA
661 and quantified. The percentage of lesions is graded as I, II, III, defined as no
662 to moderate leakage, and IV, clinically relevant leakage (n = 60 lesions of 10
663 eyes of 6 mice). Two mice eyes were excluded due to hemorrhage. **D)**
664 Volume Quantifications of the CNV lesions in flat mounts (n = 24 lesions of 4

665 eyes of 4 mice). **E)** Volume Quantifications of the fibrotic lesions in flat mounts
666 (n = 24 lesions of 4 eyes of 4 mice). *p < 0.05. Error bars are SEM.
667
668 **Figure 2: Time-dependent expression of fibrosis markers**
669 **A)** Representative hematoxylin and eosin staining of the retina-choroidal
670 complex of eye sections 7, 14, 21, 28, 35, 42 and 49 days after laser-induced
671 CNV-related fibrosis (n = 18 lesions of 3 eyes of 3 mice). Immunostaining
672 shows localizations of a-SMA (green) and type 1 collagen (red). Blue
673 indicates nuclei stained with 4,6-diamidino-2-phenylindole (DAPI). Scale bar
674 represents 50 μm. **B)** Quantification of type 1 collagen and a-SMA on all
675 designated time points (n = 18 lesions of 3 eyes of 3 mice). *p < 0.05. Error
676 bars are SEM.
677
678
679

Figure 3: Screening of different fibrosis markers of the RPE-choroid complex at the designated time post laser

A) Western blot analysis of whole-cell lysates from RPE-choroid complex of normal and CNV eyes at the indicated time points after laser injury. **B)** Quantification of type 1 collagen, **C)** Quantification of a-SMA, **D)** Quantification of fibronectin, **E)** Quantification of vimentin (10 lesions per eye, n= 3 eyes of 3 mice; grey, blue and black dots correspond to the three different western blot results obtained). Red asterisk *$p < 0.05$. Error bars are SEM.

Figure 4: Screening of different fibrosis markers in the retina at the designated time post laser

A) Western blot analysis of whole-cell lysates from retinas of normal and CNV eyes at the indicated time points after laser injury. **B)** Quantification of type 1 collagen, **C)** Quantification of a-SMA, **D)** Quantification of fibronectin, **E)** Quantification of vimentin (10 lesions per eye, n= 3 eyes of 3 mice; grey, blue

696 and black dots correspond to the three different western blot results

697 obtained). Red asterisk *p < 0.05. Error bars are SEM.

698

699

A

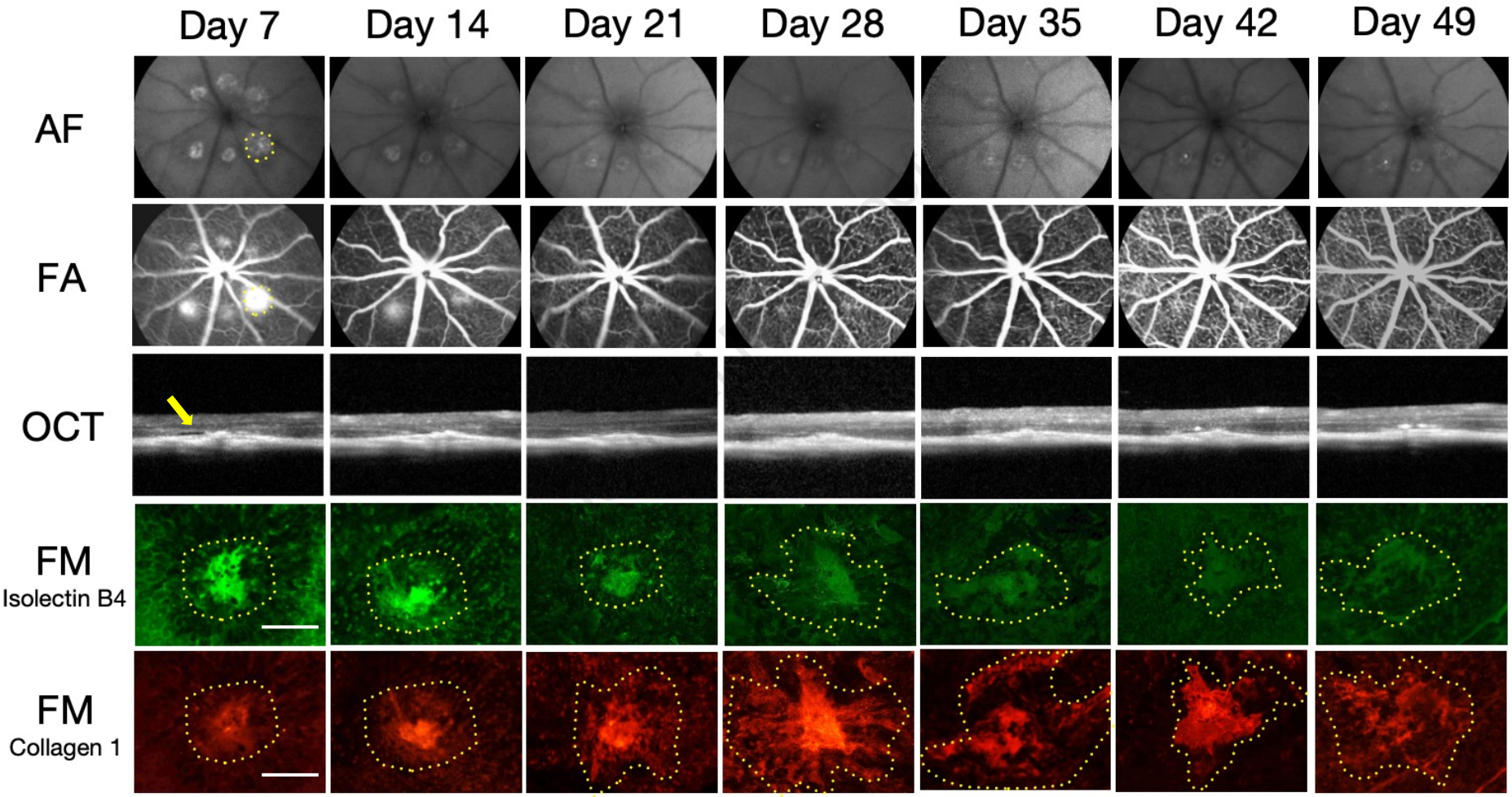

Figure 1

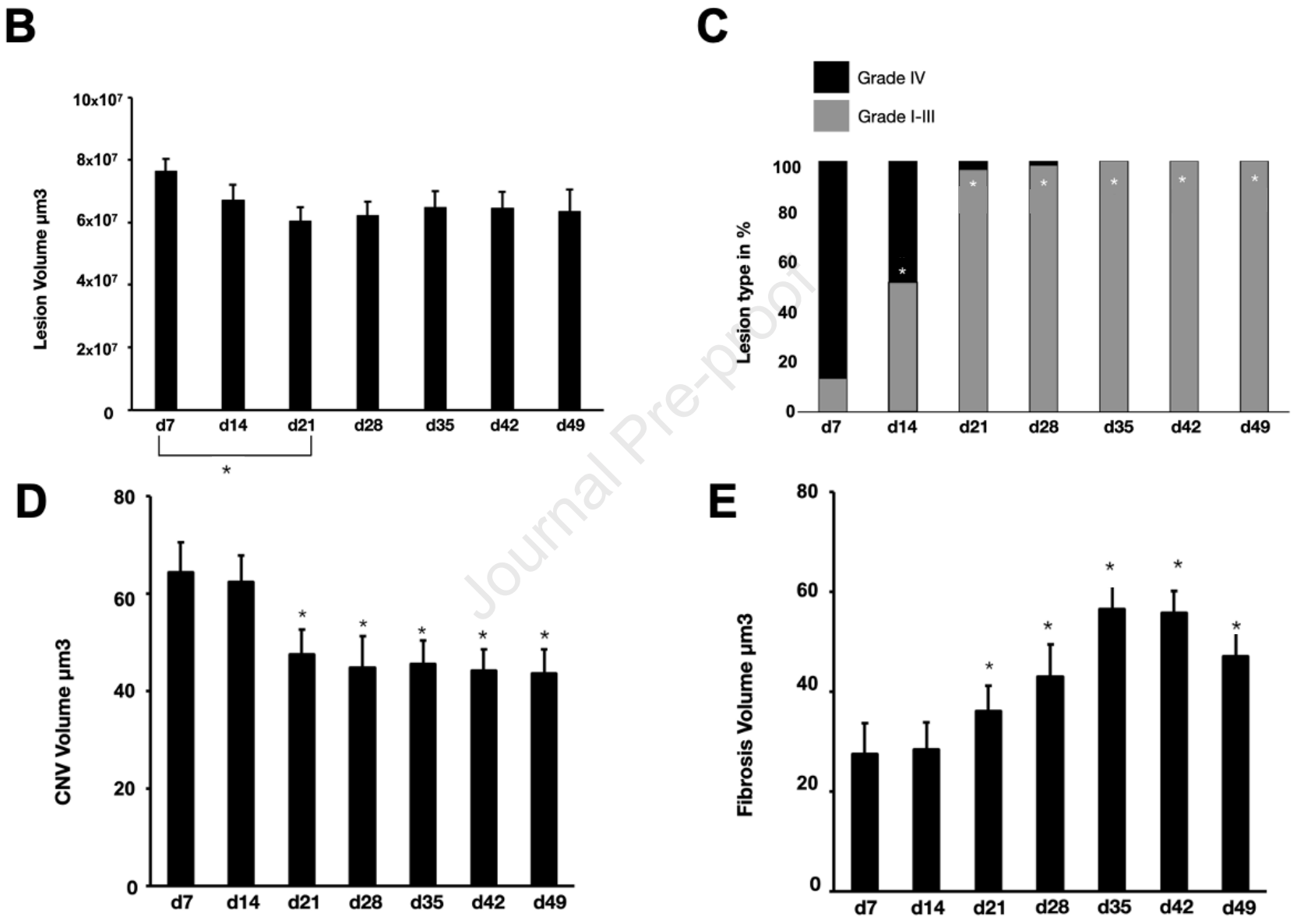

Figure 1

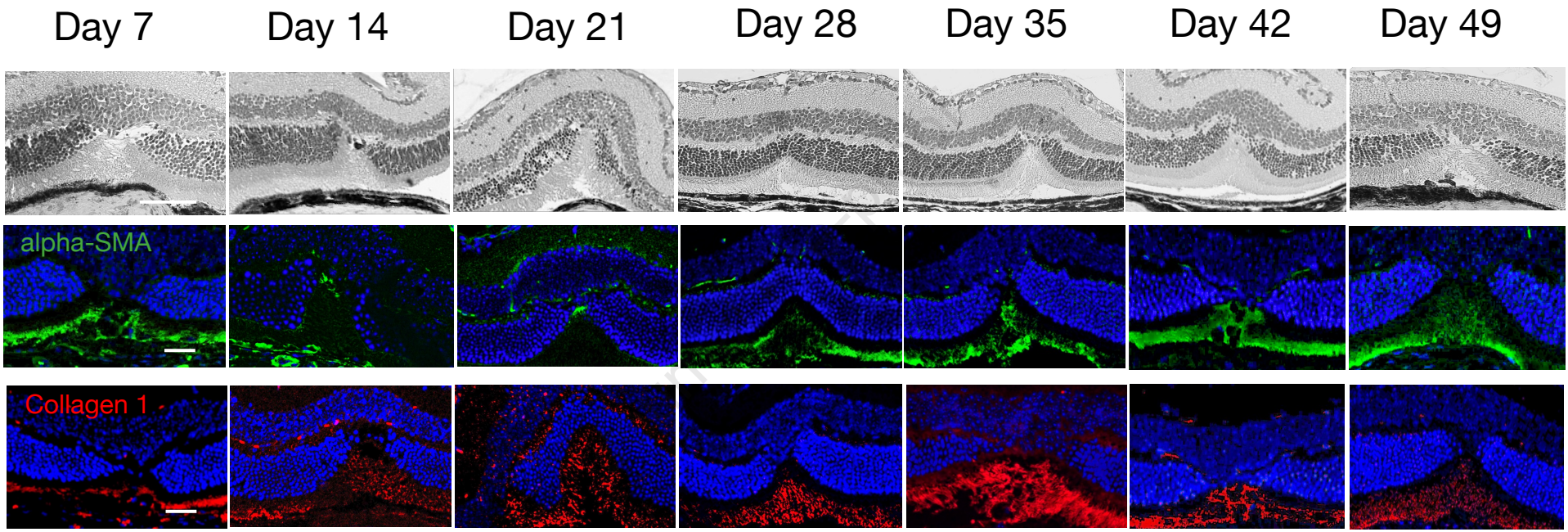

Figure 2

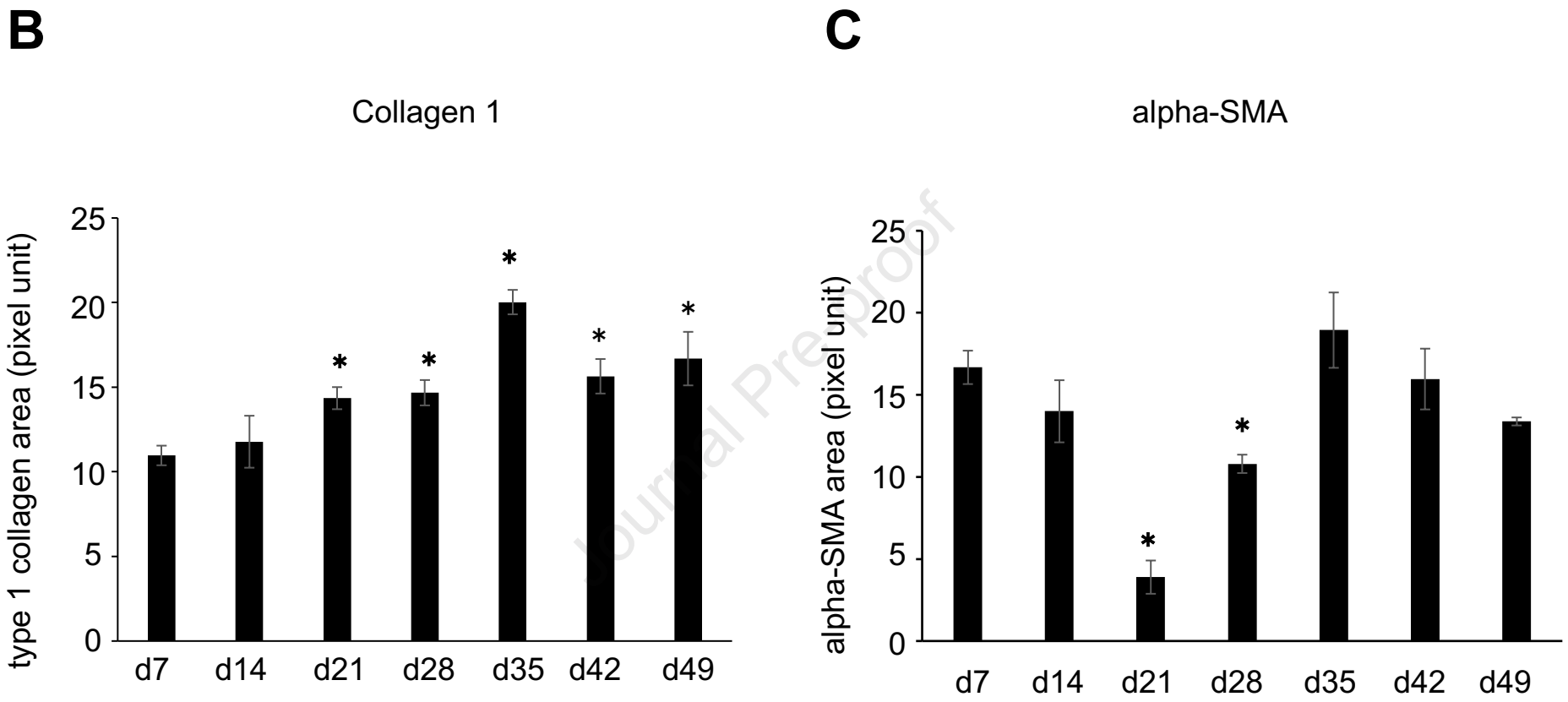

Figure 2

A

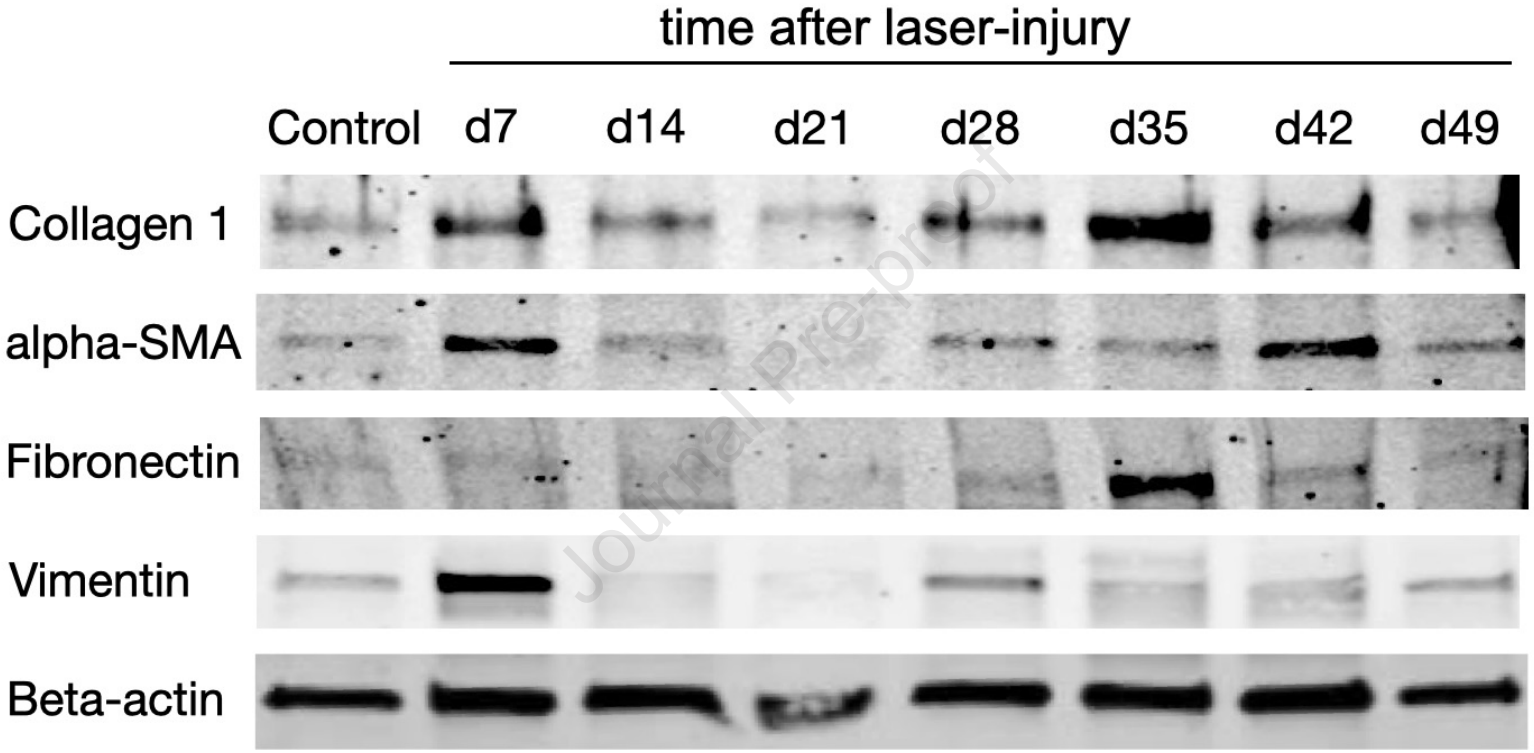

Figure 3

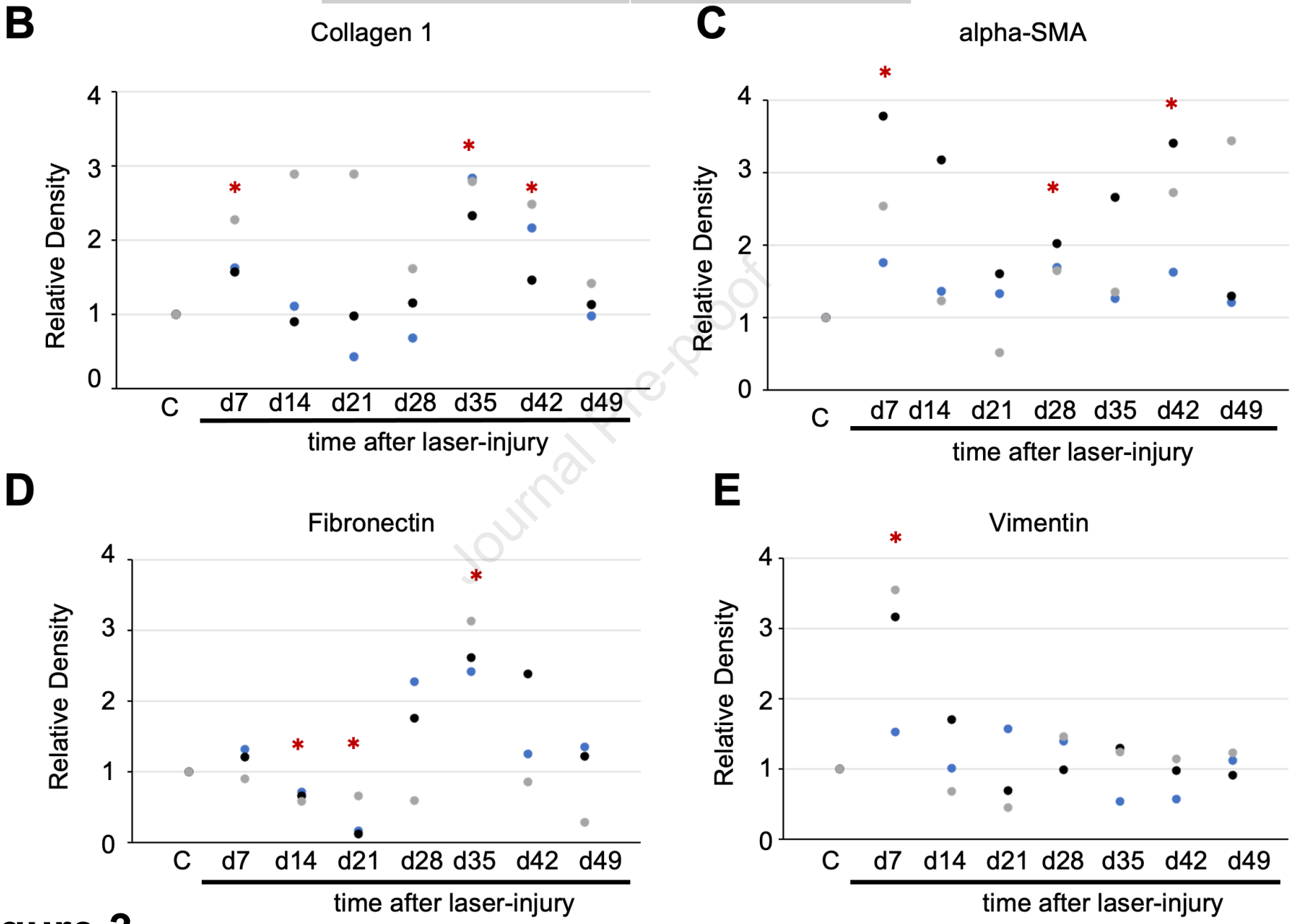

Figure 3

A

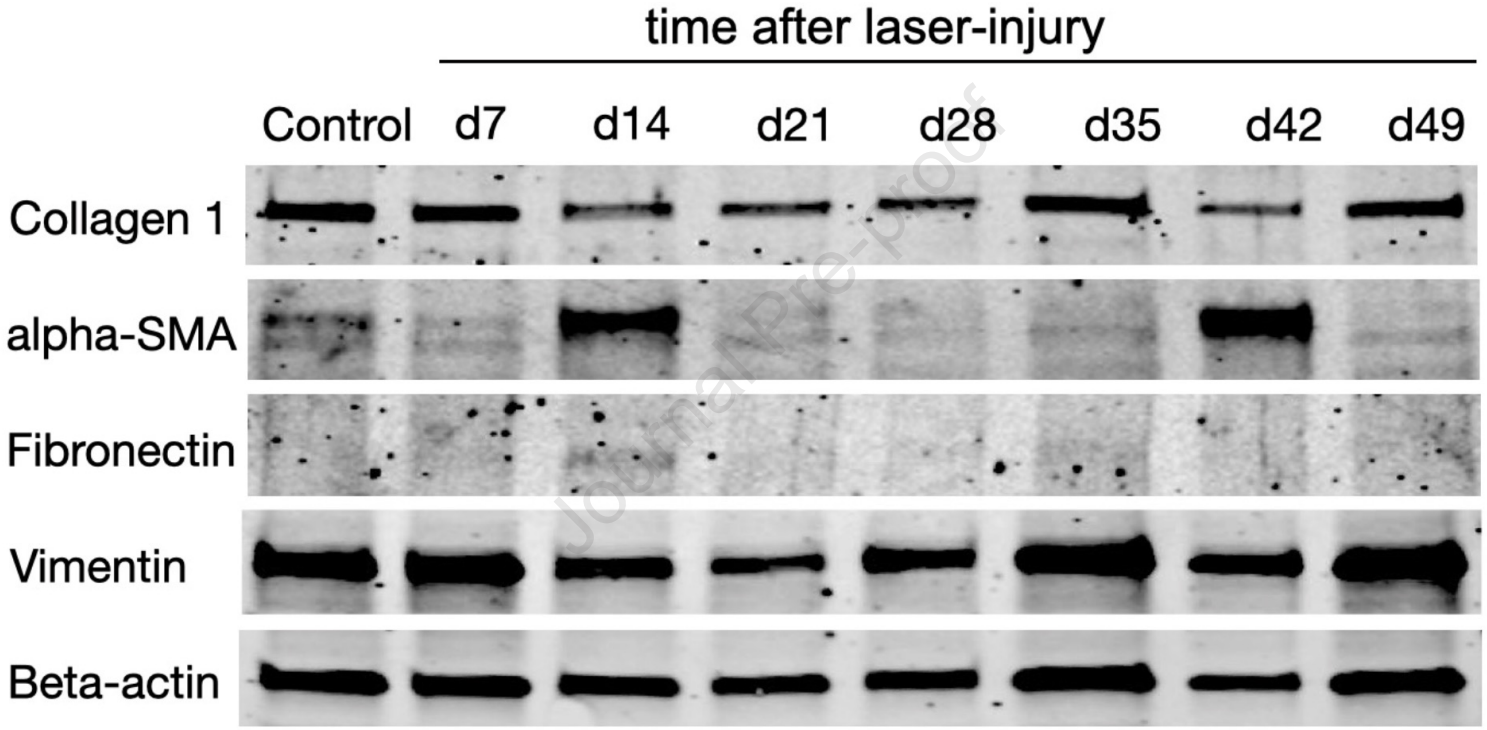

Figure 4

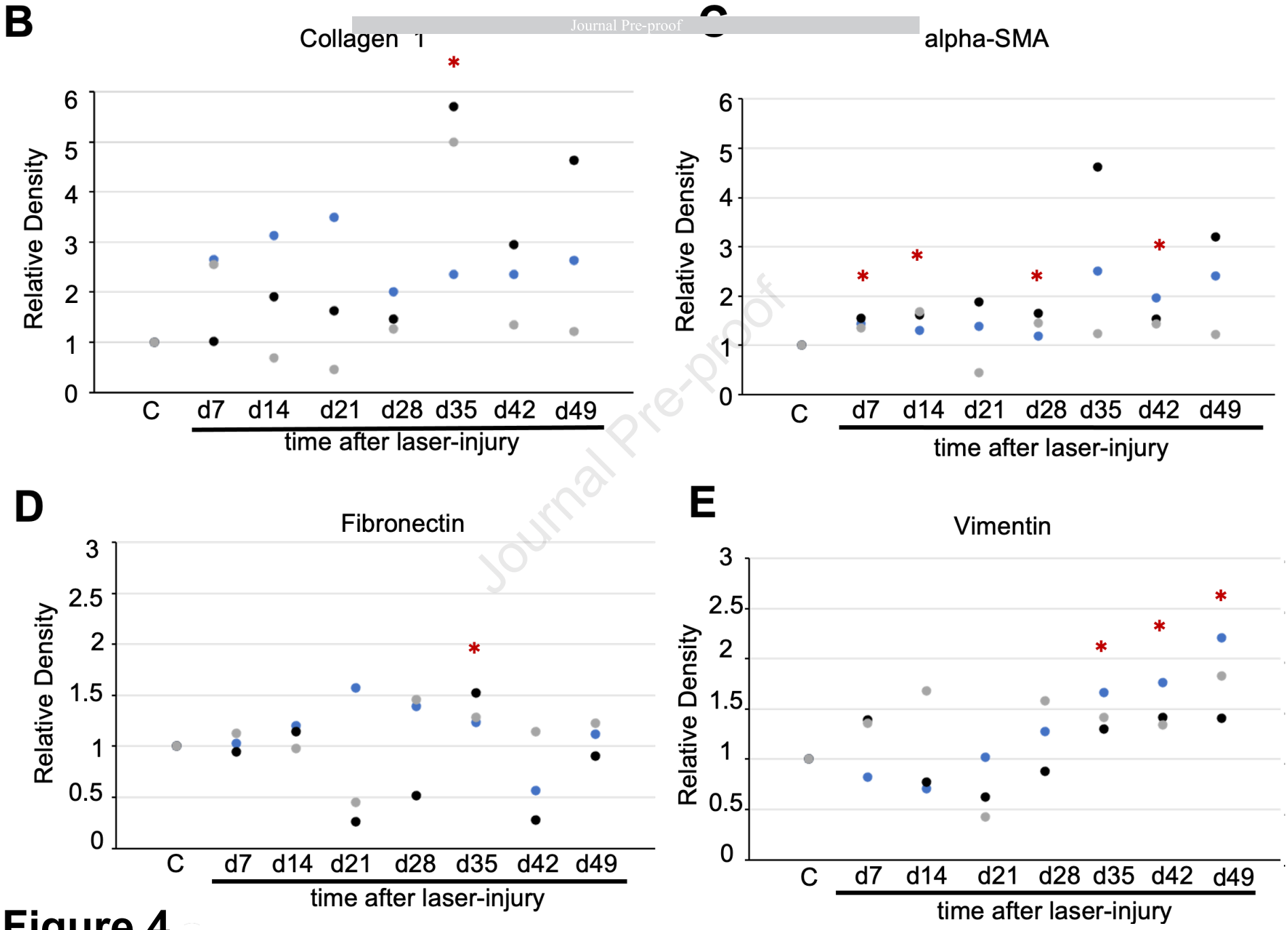

Figure 4

Highlights

- Subretinal fibrosis model of solely fibrosis
- Subretinal fibrosis without active choroidal neovascularization (CNV)
- Screen for urgently needed anti-fibrotic compounds for ocular fibrotic diseases